PROCEEDINGS of the
23rd International Congress on Acoustics

9 to 13 September 2019 in Aachen, Germany

Experimental structure intensity analysis of an Airbus A400M fuselage structure using high-resolution vibration measurements

René WINTER[1]; Simon HEYEN[2]; Jörn BIEDERMANN[3]

[1,2,3] Deutsches Zentrum für Luft- und Raumfahrt e.V., Germany

ABSTRACT

An ongoing challenge in the analysis of aircraft cabin vibrations in the mid-frequency range is the analysis of transfer paths through the complex fuselage structure. Knowing these paths would allow for simpler and more cost efficient counter measures to harmonic noise sources like engines or the auxiliary power unit.
The A400M-MSN5 fuselage structure located at the University of the Federal Armed Forces in Hamburg (HSU) is a production line A400M fuselage repurposed as a test facility for experimental studies allowing for full scale tests of novel experimental methods for acoustics and structure-born noise.
In this paper, the results of the deployment of a fully automated and autonomous Laser-Doppler-Vibrometer scanner used to measure the structure-vibration above the cabin floor at a high spatial resolution are presented. A total of more than 17000 individual measurement positions spaced approximately 9 cm apart was measured, using both a loudspeaker system and a shaker as an excitation source.
Utilizing the measured high resolution deflection shapes energy transfer paths were calculated using a hybrid Numerical-Experimental approach to structural intensity analysis.

Keywords: Structure Intensity Analysis, Vibration Measurement, Laser-Doppler-Vibrometer

1. INTRODUCTION

Detailed vibro-acoustic testing of full-scale aircraft structures is performed with different goals in mind: Updating a finite element method (FEM) model to be valid up to the highest frequencies permitted by the measurement details to get a precise prediction of a structure's low- to mid-frequency behavior(1). The validation of coupling parameters needed to calculate vibration levels in the higher frequency range using energy-based methods like statistical energy analysis (SEA) (2). In recent years structural intensity analysis (STI) came into focus as a method which can provide detailed information about the energy flow through a structure. This method is of high value if the goal is to know and maybe change the path of energy transfer, its sources and its sinks in complex structures. In case of an aircraft the transfer path of vibration originating from the engines along the structure is mostly unknown once it reaches the fuselage which is a single tubular structure with stiffeners in both circumferential and longitudinal direction with high local variations in setup.

Calculating the STI based on numerical data originating from a FEA is a more or less simple task. Using experimental data of large structures measured outside a laboratory can be challenging. Often only the out of plane vibrations are known. We proposed (3) a hybrid experimental-numerical method that already provided some very promising results (4) for a full-scale aircraft fuselage structure.

To use that method a very high density of points at which the out-of-plane vibrations of the structure are known is required, resulting in long and costly measurement campaigns if performed using accelerometers. To reduce this problem we developed a specialized, autonomous measurement system, based on a Laser-Doppler-Vibrometer (4).

In cooperation with the Helmut Schmidt University of the Federal Armed Forces in Hamburg (HSU) the German Aerospace Center (DLR) combined this system with the HSU's microphone array to setup an automated measurement system able to measure the vibration response on the upper fuselage. This system was used to autonomously perform two measurements acquiring vibrational data from loudspeaker array and shaker excitation.

After the data was validated by comparison to earlier measurements (5), it was used to calculate

[1] rene.winter@dlr.de

structural intensities. An analysis of the STI pattern provided insight into the general vibrational transfer along the structure and some deficits of the structure's environment. After performing a Hodge-Helmholtz decomposition of the STI vector field, several energy sinks were found in the STI data. These mark the positions of tuned vibration absorbers present within the structure.

2. THEORETICAL BACKGROUND

In order to identify the energy transfer from an energy source through the aircraft fuselage the structural intensity is used, which is a vectorial quantity describing the change of energy density in an infinitesimal volume (6). It is valid in time as well as in frequency domain. In time domain the structural intensity describes the instantaneous energy flow and in the frequency domain the net energy flow per frequency for steady state random vibrations.

In general, it is defined as the matrix vector product of the stress tensor $[\sigma]$ and the conjugate complex velocity vector $[v]^*$ at an arbitrary point of the structure. The velocity vector is rotated and amplified by the stress tensor.

$$\begin{bmatrix} I_x(\omega) \\ I_y(\omega) \\ I_z(\omega) \end{bmatrix} = -\Re\left(\begin{bmatrix} \sigma_{xx}(i\omega) & \sigma_{xy}(i\omega) & \sigma_{xz}(i\omega) \\ \sigma_{yx}(i\omega) & \sigma_{yy}(i\omega) & \sigma_{yz}(i\omega) \\ \sigma_{zx}(i\omega) & \sigma_{zy}(i\omega) & \sigma_{zz}(i\omega) \end{bmatrix} \begin{bmatrix} v_x(i\omega) \\ v_y(i\omega) \\ v_z(i\omega) \end{bmatrix}^* \right) \tag{1}$$

2.1 Structural Intensity of thin plates

Due to the thin-walled nature of aircraft fuselages, the structural intensity is discussed based on the theory of plates of Reissner(7) and Mindlin(8). It uses the assumption that the normal to the mid-surface remains straight for all deformations. Then it is applicable for small displacements u of the plate

$$u_x = z\varphi_y \qquad\qquad u_y = -z\varphi_x \tag{2,3}$$

with the in-plane coordinates x and y, the perpendicular coordinate of the plate z and the rotation of the normal to the undeformed mid-surface φ_x and φ_y.

Integrating the structural intensity over the thickness h of the plate and dividing by the thickness gives the averaged net energy flow I' of the plate along the mid-surface

$$I' = \frac{1}{h}\int_{-\frac{h}{2}}^{-\frac{h}{2}} I\mathrm{d}z \tag{4}$$

In this case the structural intensity can be described with the stress resultants: shear forces Q and the internal moments M with the Young's modulus E and Poisson's ratio ν:

$$Q_x = \int_{-\frac{h}{2}}^{\frac{h}{2}} \sigma_{xz}\mathrm{d}z = \frac{Eh}{2(1-\nu^2)}\epsilon_{xz} \qquad Q_y = \int_{-\frac{h}{2}}^{\frac{h}{2}} \sigma_{yz}\mathrm{d}z = \frac{Eh}{2(1-\nu^2)}\epsilon_{yz} \tag{7,8}$$

$$M_x = \int_{-\frac{h}{2}}^{\frac{h}{2}} \sigma_{xx}z\mathrm{d}z = \frac{Eh^3}{12(1-\nu^2)}(\epsilon_x + \nu\epsilon_y) \qquad M_y = \int_{-\frac{h}{2}}^{\frac{h}{2}} \sigma_{yy}z\mathrm{d}z = \frac{Eh^3}{12(1-\nu^2)}(\epsilon_y + \nu\epsilon_x) \tag{9,10}$$

$$M_{xy} = \int_{-\frac{h}{2}}^{\frac{h}{2}} \sigma_{xy}z\mathrm{d}z = \frac{Eh^3(1-\nu)}{12(1-\nu^2)}\epsilon_{xy} \tag{11}$$

The z-component of the structural intensity is neglected under the assumption that the dynamic variation of the thickness of the plate is constant. I'_x and I'_y describe the out-of-plane energy flow.

$$I'_x = -\frac{1}{h}\Re\left(M_x\dot{\varphi}_y^* - M_{xy}\dot{\varphi}_x^* + Q_x v_z^*\right) \tag{5}$$

$$I'_y = -\frac{1}{h}\Re\left(M_y\dot{\varphi}_x^* + M_{yx}\dot{\varphi}_y^* + Q_y v_z^*\right) \tag{6}$$

The in-plane energy flow of the plate is neglected because the bending of the aircraft fuselage dominates the dynamic response.

2.2 Approximation of bending and shear strains with shape functions

For the estimation of the bending and shear strains at the discrete measured point of the structure element shape functions known from the Finite Element Method(9) are used. The bending strains are defined as

$$\sigma_{xx} = -\frac{\partial\varphi_y}{\partial x} \qquad \sigma_{yy} = \frac{\partial\varphi_x}{\partial y} \qquad \sigma_{xy} = \frac{\partial\varphi_x}{\partial y} - \frac{\partial\varphi_y}{\partial x} \tag{12}$$

and the shear strains as

$$\sigma_{xz} = \frac{\partial u_z}{\partial x} + \varphi_y \qquad \sigma_{yz} = \frac{\partial u_z}{\partial y} - \varphi_x \tag{13}$$

under the assumption that the strains are constant through the thickness. There are several shape functions N available from linear, bilinear, quadratic and more. It depends on how the discrete points of the structure are connected. In general, M points of the structure are connected with M shape functions. In order to approximate the bending and shear strains at each measured point the derivatives of the shape functions and the local displacements and rotations are used

$$\begin{bmatrix}\epsilon_{xx}\\ \epsilon_{yy}\\ \epsilon_{xy}\\ \epsilon_{xz}\\ \epsilon_{yz}\end{bmatrix} = \begin{bmatrix} 0 & 0 & -\frac{\partial N_1}{dx} & \cdots & 0 & 0 & -\frac{\partial N_M}{dx}\\ 0 & \frac{\partial N_1}{dy} & 0 & \cdots & 0 & \frac{\partial N_M}{dy} & 0\\ 0 & \frac{\partial N_1}{dy} & -\frac{\partial N_1}{dx} & \cdots & 0 & \frac{\partial N_M}{dy} & -\frac{\partial N_M}{dx}\\ \frac{\partial N_1}{dx} & 0 & N_1 & \cdots & \frac{\partial N_M}{dx} & 0 & N_M\\ \frac{\partial N_1}{dy} & -N_1 & 0 & \cdots & \frac{\partial N_M}{dy} & -N_M & 0 \end{bmatrix} \begin{bmatrix} u_{z,1}\\ \varphi_{x,1}\\ \varphi_{y,1}\\ \vdots\\ u_{z,M}\\ \varphi_{x,M}\\ \varphi_{y,M}\end{bmatrix} \tag{14}$$

2.3 Approximation of rotation degree of freedom

Knowing that bending dominates the aircraft fuselage response the rotation degree of freedom can be derived directly by the measured bending response. Under the assumption of small displacements, the rotation can be approximated by the derivatives of the shape functions and the bending u_z

$$\varphi_x = \frac{\partial u_z}{\partial y} = \left[\frac{\partial N_1}{\partial y}\cdots\frac{\partial N_M}{\partial y}\right]\left[u_{z,1}\cdots u_{z,M}\right]^T \tag{15}$$

$$\varphi_y = -\frac{\partial u_z}{\partial x} = \left[\frac{\partial N_1}{\partial x}\cdots\frac{\partial N_M}{\partial x}\right]\left[u_{z,1}\cdots u_{z,M}\right]^T \tag{16}$$

2.4 Discrete Hodge-Helmholtz field decomposition

Most of structures show areas of local energy exchange for example between two neighboring eigenmodes. This energy exchange creates local vortices in the intensity flow field. So, the identification of the irrotational intensity flow field has significant advantages because it describes the energy flow without the masking effects of vortices that are related to the solenoidal intensity flow field (10).The intensity vector field $\vec{I}$ can be separated into an irrotational ∇E part resulting from the scalar potential E. This vector field allows for a simple identification of energy sinks and sources. An additional solenoidal (divergence-free) $\nabla\times\vec{W}$ part, showing the lossless energy flow and a harmonic remainder $\vec{R}$ are also part of the results using a discrete Hodge-Helmholtz field decomposition (11)

$$\vec{I} = (\nabla E) + \left(\nabla\times\vec{W}\right) + \vec{R} \tag{16}$$

3. Experimental Setup

The A400M acoustics fuselage demonstrator (see Figure 1) is setup at the Helmut Schmidt University (HSU) of the Federal Armed Forces in Hamburg. It is used as a test structure for new acoustic and vibro-acoustic methods and developments. The demonstrator is a production line Airbus A400M fuselage, based on an early design slightly different to the final aircrafts of this type.

Figure 1 – A400M-MSN5 Fuselage Demonstrator

Figure 2 – Inside view with measurement system

As can be seen in Figure 2 the fuselage is a ribbed cylindrical structure. The stiffeners in longitudinal direction are called stringers. The ones running perpendicular to the stringers are called frames. In this case the frame's shape above the cargo floor identifiable in figure 2 is roughly circular. The parts of the fuselages aluminum skin in between the stiffeners are called skin fields.

3.1 Equipment information

HSU and DLR setup an automated measurement system able to autonomously measure the vibrational and acoustic response at thousands of points on the upper fuselage. This was done by combining parts of DLR's 'Fuselage Laser Scanner' (FLS) with the HSU's motorized microphone array build into the A400M fuselage.

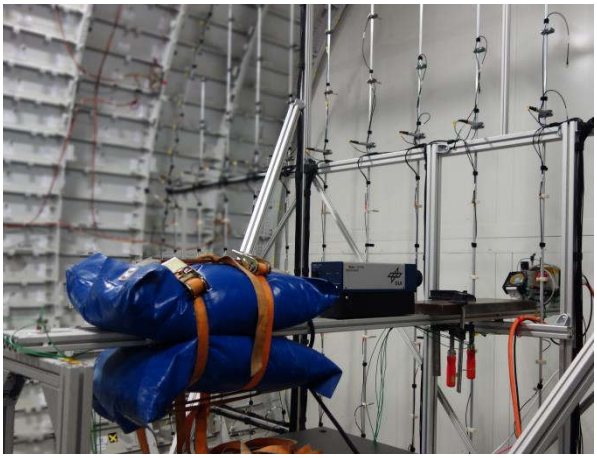

Figure 3 – The stripped down FLS setup in the center of the HSU microphone array

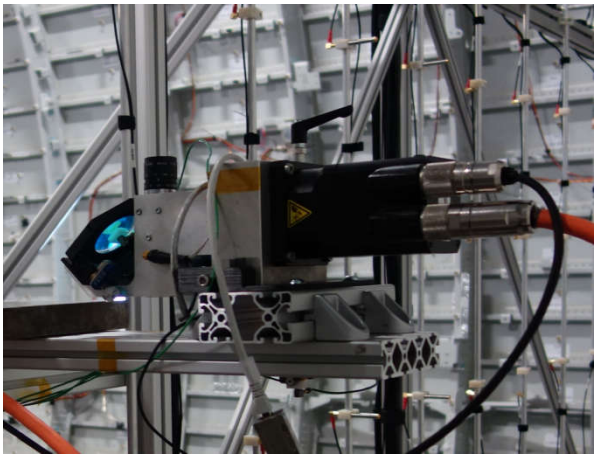

Figure 4 – Closer look at the scanning unit with mirror and camera attached to a motor

A stripped down version of the FLS, only incorporating the radial scanning unit, was mounted at the center of the motorized microphone array and thus at the center of the A400Ms radial upper section. Longitudinal movement was archived by incorporating the HSU microphone array motor into the FLS system software.

The FLS utilizes a single-point Laser-Doppler-Vibrometer (LDV, PolyTec OFV-505) mounted at one end of an aluminum beam. At the opposing end of the beam a scanning unit carrying a mirror and a digital camera (AVT Mako G-032 Mono 12) are placed. The mirror steers the laser beam in radial direction while the camera is aligned with the mirror to show the laser dot and its surroundings.

To measure the excitation signal emitted from the speaker setup PCB Type 352C22 accelerometers where placed directly on the membrane of one subwoofer of the array. A PCB 288D01 impedance sensor was used at the driving point of the shaker for acceleration and force measurement during shaker excitation.

3.2 Test procedure

The system was used to perform two autonomous measurements to acquire vibrational data containing information for the low and mid-frequency range on thousands of measurement points using two different excitation setups. During the first measurement a 12 channel subwoofer array provided by the HSU was used for acoustic excitation. For the second measurement an electromagnetic shaker with a force output of up to 200N was attached to the structure. The same band-limited random signal of 40 Hz to 400 Hz was used as excitation signal in both measurements.

A measurement grid was designed consisting of 17514 individual measurement points spreading over 126 circular sections above floor level with 139 measurement positions each. This grid spans approximately 13m of the fuselage, limited only by the movement range of the motorized microphone array. By marking 12 points of the actual A400M fuselage structure using QR markers the FLS is able to calibrate its positon automatically, measuring the 17514 individual points with a positioning precision of well below 5mm.The acquisition time at each point was set 15s to allow a measurement to be completed within 4 days even if a problem occurs and some user interaction was necessary.

4. Results

The results presented below where calculated using the available vibration data of the FLS deployment to the A400M-MSN5 fuselage. Time data was acquired at a sample rate of 3200 Hz. Structural excitation was achieved using the aforementioned excitations setups of a 12 channel subwoofer array and a single electromagnetic shaker. For this analysis frequency response functions (FRFs) were estimated using a resolution of 1 Hz, Welch's method with a Hanning Window and 70% overlap. The frequency response was calculated within the full range of excitation of 40-400 Hz.

4.1 Operational deflection shapes

Operational deflection shapes (ODS) can serve a variety of purposes, especially when analyzing a structure's response during operation or to an operation-like excitation pattern. In this case the ODS are used as a basis for the STI analysis presented below. Examining the structure's response after data processing a drawback of the automated measurements became apparent. The FLS is indifferent towards any structural details like inconsistencies not represented in the predefined measurement grid or cables installed for various purposes. A lot of the 17514 measurement positions were not actually located on the structure itself, but on non-structural or attached elements. A software was created allowing the clean-up of the acquired data utilizing both the low-frequency phase comparison between excitations and response signal and the camera image available for each measurement point. The result can be seen in Figure 5 and Figure 6. It can be seen, that the undesired data from inconsistencies vanish

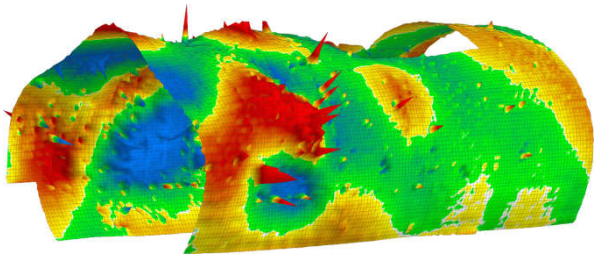

Figure 5 – ODS at 84 Hz before clean-up

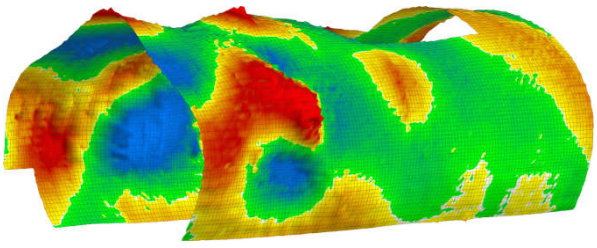

Figure 6 – ODS at 84 Hz after clean-up and interpolation (976 points removed)

and only the results of the fuselage structure remain. Of the 17514 measurement positions 980 had to be removed due to measurement errors. To reconstruct the results on the full surface area a local interpolation method based on a nearest neighbor approach was used.

To gain further insight into the validity of the measured data, a comparison with measurements of a previous campaign at the same structure can be made. That campaign was conducted in 2014 (5, 12) using a rowing sensor grid method to generate comparatively dense (approx. 1 sensor every 25 cm) vibrational data using accelerometers. The results of the comparison are shown in Figure 7 and Figure

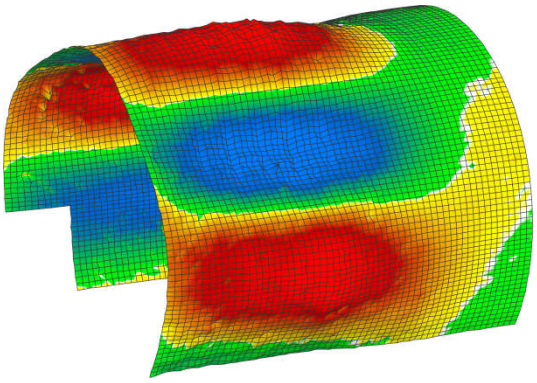

Figure 7 – ODS at 62 Hz acquired by FLS

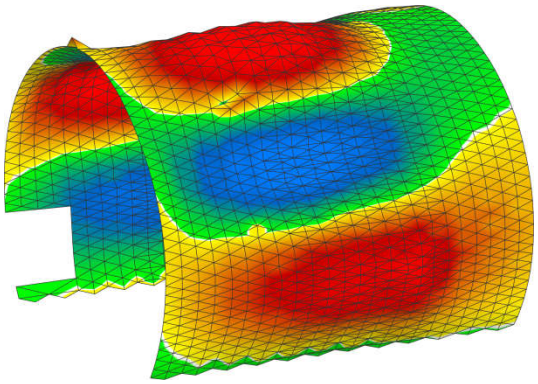

Figure 8 – ODS at 65 Hz acquired with accelerometers

8.

The operational deflection shapes at 62 Hz (FLS) and 65 Hz (Accelerometer) shown look superficially similar. Several differences need to be pointed out: Since the measurements in 2014 several structural changes were applied to the A400M acoustics fuselage demonstrator, resulting in the notable frequency shift and a slight change in the overall response shape. Most importantly a cargo-door mockup was installed closing the cavity, in addition to the combined FLS and microphone array system and an array of 'tuned-vibration-absorbers' or TVAs all of which add some considerable weight to the structure. In addition previously installed acoustic boundaries that were attached directly to the structure were removed. This further changed the dynamic characteristics of the structure.

4.2 Structural Intensity Analysis

In Figure 9 and Figure 10 the operational deflection shapes at 101 Hz are shown for both subwoofer array and shaker excitation. These two ODS are the basis for the STI analysis shown below. As is

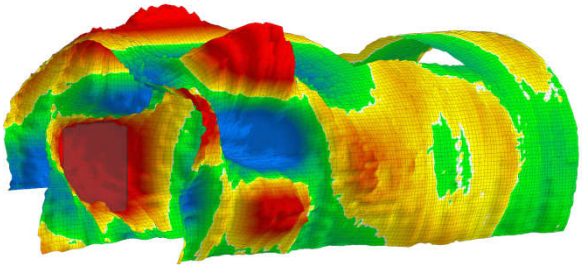

Figure 9 – ODS at 101 Hz with loudspeaker excitation

Loudspeaker position: grey rectangle

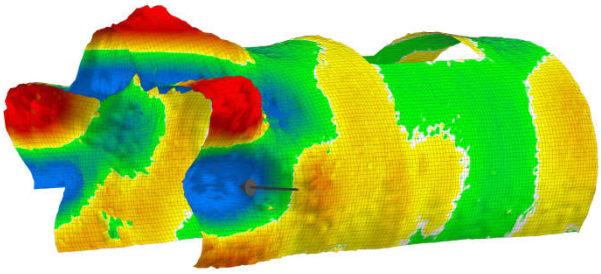

Figure 10 – ODS at 101 Hz with shaker excitation

Shaker position: grey arrow

expected both ODS show the same general shape in terms of nodal lines in circumferential and longitudinal direction, 8 and 5 respectively. The amplitudes are vastly different depending on the excitation point.

By applying the structural intensity analysis as described in chapter 2 to the frequency domain data (Figure 9 and Figure 10) it is possible to get an impression of the energy flow through the A400M-MSN5 structure during excitation at 101 Hz. The result is shown in Figure 11 and Figure 12.

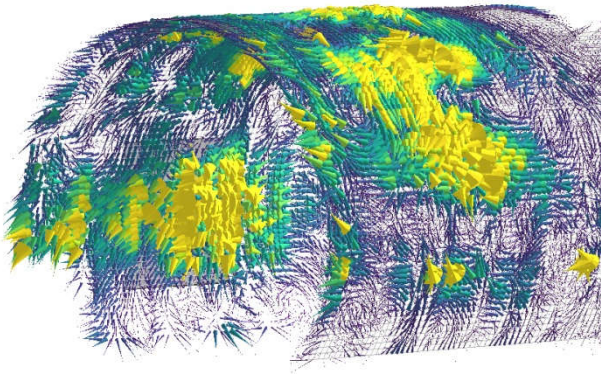

Figure 11 – STI at 101 Hz with loudspeaker excitation

Loudspeaker position: grey rectangle

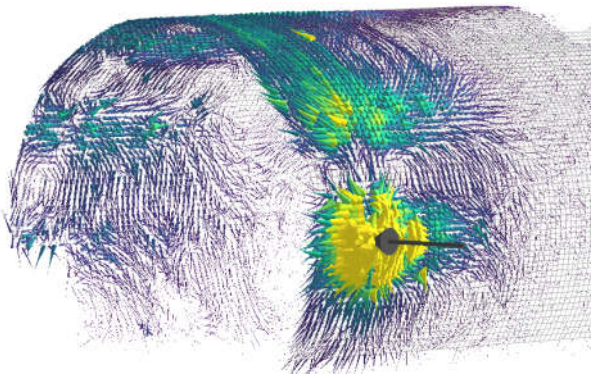

Figure 12 – STI at 101 Hz with shaker excitation

Shaker position: grey arrow

Compared to a similar analysis performed with a comparable structure and dataset (3) the results are harder to interpret. Some components potentially crucial to a full view of the transfer were not

measured: The floor, its support structure and the fuselage below floor level are not visible to the LFS. The microphone setup is optimized for a sound field reconstruction method the results of which are not available yet. The intensity levels caused by the single point shaker excitation as shown in Figure 12 seem viable. The energy spreads from the point of origin more or less evenly along the structure with the stiffened floor section and wing-box section acting as barriers.

The intensity levels caused by the acoustic excitation are more random with high energy inflow outside the sources sound field. This is most likely caused by reflections within the laboratory, which is highly reverberant to all but the front side of the fuselage. While these effects are also present for the shaker excitation, they are comparatively low due to the reduced relative amplitudes. The shaker causes a sound field within the laboratory only as an effect of the vibrating fuselage surface.

By decomposing the vector field into its irrotational and solenoidal components (see Figure 13 - Figure 16) the net energy flow becomes easier to identify. One particular feature of the irrotational vector field shown in Figure 13 and Figure 14 are a couple of energy sinks, marked by intensity cones

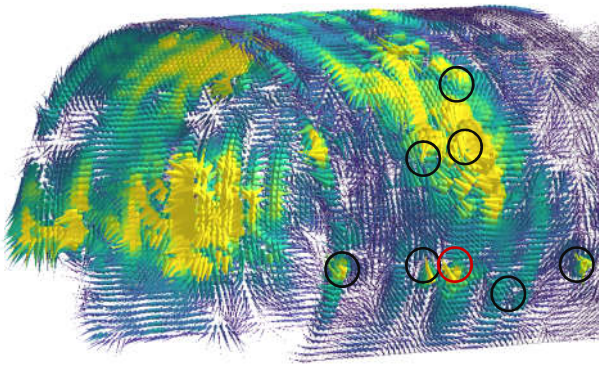

Figure 13 – Irrotational field of STI at 101 Hz with loudspeaker excitation, circles show energy sinks

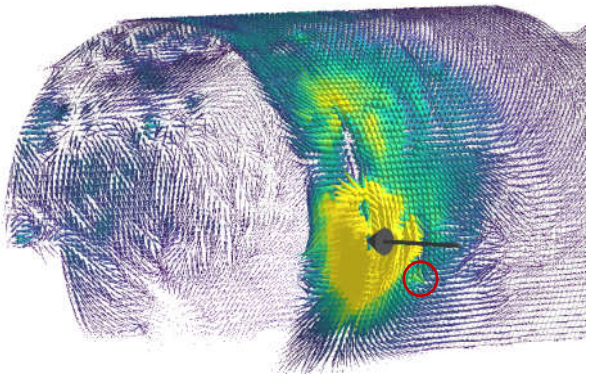

Figure 14 - Irrotational field of STI at 101 Hz with shaker excitation, red circle shows energy sink

pointing towards each other. It is at these positions that the structure is fitted with TVAs. Though switched off, they are still supposed to have a damping effect at a single frequency. While the loudspeaker excitation shows eight of approximately 25 TVA positions in the field of view only a single one is seen with shaker excitation. This one is present in both plots. This might be caused by a visual masking effect resulting from the two orders of magnitude higher vibration level of the shaker excitation.

The solenoidal vector fields are shown in Figure 15 and Figure 16. When superimposed with the irrotational fields above they would result in the undecomposed fields. The solenoidal fields show energy exchange of modal responses of the structure close to 101 Hz.

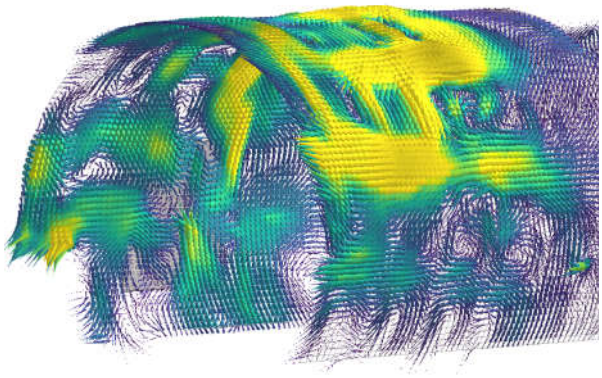

Figure 15 – Solenoidal field of STI at 101 Hz with loudspeaker excitation

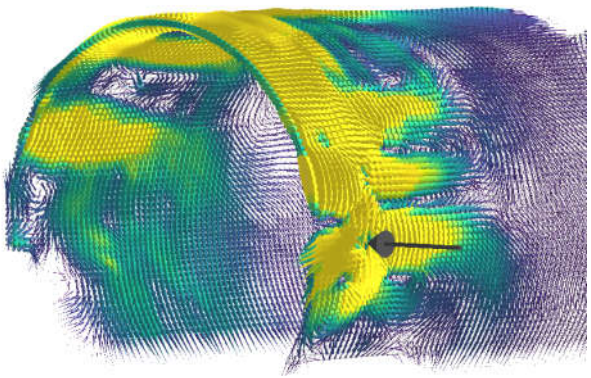

Figure 16 - Solenoidal field of STI at 101 Hz with shaker excitation

5. SUMMARY

Using the fully automated LFS measurement system to acquire vibrational data at a full-sized aircraft fuselage yielded good results in terms of data quality. The biggest drawback when compared to manual measurements is the systems indifference to local structural inconsistencies or previously unknown attachments. This can in principle easily be solved by a preliminary measurement run to manually fine tune the grid before doing the final measurements. Alternatively, the systems capabilities could be enhanced by incorporating online verification based on measurement data and camera images to slightly modify the measured grid during measurements.

The STI analysis resulted in reasonable results, not only showing a likely spread of vibrational energy through the structure emanating from the two different excitation systems, but also allowing the identification of the position of some of the structural dampeners built into the A400M-MSN5 test facility by clearly marking them as energy sinks.

ACKNOWLEDGEMENTS

The data forming the basis for the analysis presented here has been acquired in the joint research project Flight-LAB within the fifth Aeronautical Research Program (LuFo V). The project is funded by the Federal Ministry for Economic Affairs and Energy on the basis of a decision by the German Bundestag.

REFERENCES

1. Tengzelius U, Horlin N, Emborg U, Gustavsson M, der Auweraer HV, Iadevaia M. Correlation of medium frequency test and FE models for a trimmed aircraft test section. Aeroacoustics Conferences: American Institute of Aeronautics and Astronautics; 1998. p. -.
2. Fahy FJ, Price WG, Keane AJ. Statistical energy analysis: a critical overview. Philosophical Transactions of the Royal Society of London Series A: Physical and Engineering Sciences. 1994;346(1681):431-47.
3. Biedermann J, Winter R, Norambuena M, Böswald M. A hybrid numerical and experimental approach for structural intensity analysis of stiffened lightweight structures. ISMA2018.
4. Winter R, Biedermann J, Norambuena M. High-Resolution Vibration Measurement And Analysis Of The Flight-LAB Aircraft Fuselage Demonstrator. INTER-NOISE2018.
5. Winter R, Biedermann J, Böswald M, Wandel M. Dynamic characterization of the A400M Acoustics Fuselage Demonstrator. INTER-NOISE2016. p. 3296-306.
6. Gavrić L, Pavić G. A Finite Element Method for Computation of Structural Intensity by the Normal Mode Approach. Journal of Sound and Vibration. 1993;164(1):29 - 43.
7. Reissner E. On the theory of transverse bending of elastic plates. International Journal of Solids and Structures. 1976;12(8):545 - 54.
8. Mindlin RD. The effect of transverse shear deformation on the bending of elastic plates. Journal of Applied Mechanics. 1951;18:31-8.
9. Bathe K-J. Formulation and Calculation of Isoparametric Finite Element Matrices. In: Strenquist W, Peterson M, editors. Finite Element Procedures1996.
10. Roozen NB, Guyader JL, Glorieux C. Measurement-based determination of the irrotational part of the structural intensity by means of test functional series expansion. Journal of Sound and Vibration. 2015;356:168-80.
11. Guo Q, Mandal MK, Li MY. Efficient Hodge–Helmholtz decomposition of motion fields. Pattern Recognition Letters. 2005;26(4):493-501.
12. Winter R, Norambuena M, Biedermann J, Böswald M. Experimental characterization of vibro-acoustic properties of an aircraft fuselage. ISMA2014. p. 2731-48.